JUNE 1978 PPPL-1452
UC-20g

NONLINEAR EVOLUTION OF LOWER HYBRID WAVES

BY

C. F. F. KARNEY, A. SEN,
AND F. Y. F. CHU

PLASMA PHYSICS LABORATORY

MASTER

DISTRIBUTION OF THIS DOCUMENT IS UNLIMITED

DEI SUB NUMINE VIGET

PRINCETON UNIVERSITY
PRINCETON, NEW JERSEY

This work was supported by the U. S. Department of Energy Contract No. EY-76-C-02-3073.

Nonlinear Evolution of Lower Hybrid Waves

by

Charles F. F. Karney

Plasma Physics Laboratory, Princeton University, Princeton, NJ 08540

Abhijit Sen

Plasma Fusion Center, Massachusetts Institute of Techn gy, Cambridge, MA 02139

and

Flora Y. F. Chu

Electronic Systems Laboratory and Department of Electrical Engineering and Computer Science,

Massacusetts Institute of Technology, Cambridge, A 02139

Abstract

The two-dimensional steady-state distribution of lower hybrid waves is governed by the complex modified Korteweg-deVries equation, $v_\tau + v_{\xi\xi\xi} + (|v|^2 v)_\xi = 0$, where v is proportional to the electric field and ξ and τ are two spatial coordinates. The equation is studied numerically. Two types of solitary waves can arise. One is a constant phase pulse, whereas the other is an envelope solitary wave. These solitary waves are not solitons. The occurrence of the constant phase pulses points to the possibility of internal reflections due to scattering off ponderomotive density fluctuations. This necessitates solving the equation as a boundary value problem. With typical fields for lower hybrid heating of a tokamak, it is found that large reflections can occur close to the edge of the plasma.

I. INTRODUCTION

In typical lower hybrid heating schemes, lower hybrid waves are launched at the wall of a tokamak by an array of waveguides, and must propagate into the center of the plasma in order to heat it. Because of the high fields required, nonlinear effects on the propagation are important. This problem was first tackled by Morales and Lee[1] who considered the two-dimensional steady-state propagation of one of the two lower hybrid rays in a homogeneous plasma. By considering the balance between thermal dispersion and the self-modulation due to the ponderomotive force they derived what has become to be known as the complex modified Korteweg-deVries (CMKDV) equation.

This equation is not analytically soluble. In this paper we study the CMKDV equation numerically, and determine the consequences of our results for lower hybrid heating.

The plan of this paper is as follows: Section II explains the origin of the CMKDV equation, and its relation to the modified Korteweg-deVries (MKDV) equation and other soluble equations. In Sec. III we present the known constants of the motion for the CMKDV equation. There are only a finite number of these indicating that it is not analytically soluble. We consider in Sec. IV the evolution of pulses numerically, and show that a pulse can break up into two types of solitary waves, constant phase pulses or envelope pulses. We examine the properties of these two types of solitary pulses in more detail in Secs. V and VI and show how they are related to the solitons of the MKDV equation. In Sec. VII we examine the results of Sec. IV in the light of Secs. V and VI and make some general remarks about the evolution of pulses. Because of the appearance of constant phase pulses, which indicates that nonlinear reflection is occurring, we consider the CMKDV equation as a boundary value problem (Sec. VIII), which we solve numerically. Section IX applies our results to the problem of lower hybrid heating of a tokamak.

II. THE CMKDV EQUATION

The two-dimensional steady-state propagation of a single lower hybrid ray in a homogeneous plasma is governed by[1]

$$v'_{\tau'} + v'_{\xi'\xi'\xi'} + (|v'|^2 v')_{\xi'} = 0\,, \tag{1}$$

where subscripts denote differentiation and

$$v' = \left(\frac{\varepsilon_0}{4n_0(T_e + T_i)}\right)^{1/2} \tilde{E}_x^* , \tag{2}$$

$$\xi' = (x - gz)/A , \tag{3}$$

$$\tau' = x/(2K_\perp A) , \tag{4}$$

and $E_x(x, z, t) = \mathrm{Re}[\tilde{E}_x(x, z)\exp(-i\omega t)]$, x and z are the coordinates perpendicular and parallel to the magnetic field, $g = (-K_\perp/K_\parallel)^{1/2}$. The components of the cold plasma dielectric tensor are given as $K_\perp = 1 + \omega_{pe}^2/\Omega_e^2 - \omega_{pi}^2/\omega^2$, $K_\parallel = 1 - \omega_{pe}^2/\omega^2$ where Ω_e is the electron gyrofrequency and ω_{pj} are the electron ($j = e$) and ion ($j = i$) plasma frequencies. The coefficient A is due to thermal dispersion and is given by $A^2 = 3\lambda_{De}^2[1 - \frac{1}{3}(\omega_{pe}/\Omega_e)^2 + \frac{1}{4}(\omega_{pe}/\Omega_e)^4 + (T_i/T_e)(\omega_{pi}/\omega)^4]$. For convenience we will introduce an additional scaling of the variables,

$$v = \lambda v' , \ \xi = \lambda^{-1}\xi' , \ \tau = \lambda^{-3}\tau' . \tag{5}$$

Equation (1) is invariant under this scaling and so reads

$$v_\tau + v_{\xi\xi\xi} + (|v|^2 v)_\xi = 0 , \tag{6}$$

the complex modified Korteweg-deVries (CMKDV) equation. This transformation is useful, since we can pick λ in such a way that the representative scale length in ξ is unity. Two other transformations which leave (6) invariant are

$$v \to v^* , \ v \to v\exp(i\theta_0) , \tag{7}$$

where θ_0 is a constant.

The physical meaning of the terms in (6) are as follows: If only the first term were present the solution would be $v(\tau, \xi) = v(\xi)$. This describes the propagation of the lower hybrid waves along the right-going ray ($x = gz$), and is an accurate description in the linear long-wavelength limit ($v \to 0$, $\partial/\partial\xi \to 0$). The second term causes the lower hybrid waves to disperse due to thermal effects. The third term causes self-modulation and arises because the plasma density is reduced in the region of finite v by an amount proportional to the square of the electric field, and so the propagation characteristics of the waves are altered.

We note that (6) describes the nonlinear evolution of plasma waves in other frequency ranges.[2] More generally the CMKDV equation describes the steady-state [time dependence ~ $\exp(-i\omega t)$] two-dimensional (x and z) propagation of electrostatic waves in a homogeneous anisotropic medium which is invariant to the transformation, $x \to -x$, $z \to -z$, and whose dielectric tensor depends on the square of the electric field. The medium must be non-dissipative and must support propagating electrostatic waves. The relative signs of the nonlinear and dispersive terms in (6) may differ, which would lead to important differences in the solution.

Equation (6) is closely related to the modified Korteweg-deVries (MKDV) equation

$$v_\tau + v_{\xi\xi\xi} + \kappa|v|^2 v_\xi = 0\,, \tag{8}$$

where κ is a positive constant. The importance of this equation lies in the fact that it is soluble by the *inverse scattering method*[3,4] (see Appendix). The solution generally consists of several solitons together with some radiation. As $\tau \to \infty$, the radiation decays due to the action of the dispersive term in (6), leaving just the solitons. The distinguishing property of the solitons is that apart from a shift in their position and phase they are unaltered by collisions with other solitons or with the radiation. To see the relation between (6) and (8) we write (6) in two other ways,

$$v_\tau + v_{\xi\xi\xi} + 3|v|^2 v_\xi = 2i|v|^2 v\,\theta_\xi\,, \tag{9}$$

where $\theta = \arg(v)$, and

$$v_\tau + v_{\xi\xi\xi} + |v|^2 v_\xi = -v|v^2|_\xi\,. \tag{10}$$

Thus in two limits the CMKDV equation reduces to the MKDV equation: Firstly if the phase variation of v is small, i.e. $\theta_\xi \ll (\log|v|)_\xi$, then the right hand side of (9) may be neglected, giving (8) with $\kappa = 3$. On the other hand if the phase variation of v is large, i.e. $\theta_\xi \gg (\log|v|)_\xi$, then the right hand side of (10) may be neglected giving (8) with $\kappa = 1$. Note that the relative strengths of the nonlinear terms are different in these two limits.

These two limits have been recognized by others. Morales and Lee[1] considered the case when v is real (a special case of slow phase variation) in which case (6) becomes the real modified Korteweg-deVries (RMKDV) equation. However the definition of v shows that it is generally complex. Furthermore it may be shown[5] that the case where v is purely real is inapplicable to the problem of excitation of lower hybrid rays from a source. This may be understood from the following considerations. The energy density of lower hybrid waves is proportional to $|\tilde{E}_x(k_z)|^2$, and the group velocity of the right-going ray is proportional to $1/k_z$. Therefore the power flow of a spectral component of the wave is proportional to $|v(k)|^2/k$, where k is the Fourier-transform variable conjugate with ξ. If v is purely real, there will be no net power flow, because $|v(k)| = |v(-k)|$. If we impose the condition that all the spectral components of v carry power into the plasma at $\tau = 0$, then we require that $v(0, k < 0) = 0$, or[5]

$$\begin{aligned} v(0, \xi) &= F^{-1}\{u(k)F[w(\xi); \xi, k]; \xi, k\} \\ &= \frac{1}{2}\, w(\xi) + \frac{1}{2\pi i} \ \mathrm{P}\!\!\int_{-\infty}^{\infty} \frac{w(\xi')}{\xi' - \xi}\, d\xi' , \end{aligned} \tag{11}$$

where F is the Fourier-transform operator and u is the unit step function.

The limit of rapid phase variation was treated by Newell and Kaup.[6] Making the following changes of variables, $v(\tau, \xi) = \sqrt{6}\, u(\eta, \zeta)\exp[i(k_0\xi + k_0^3\tau)]$, $\zeta = \xi + 3k_0^2\tau$, $\eta = 3k_0\tau$, in (6) they obtained

$$u_\eta + iu_{\zeta\zeta} + 2i|u|^2u + u_{\zeta\zeta\zeta}/(3k_0) + 2(|u|^2u)_\zeta/k_0 = 0 . \tag{12}$$

In the limit of $|u_\zeta/u| \ll k_0$, (12) reduces to the nonlinear Schrödinger (NLS) equation,

$$u_\eta + iu_{\zeta\zeta} + 2i|u|^2u = 0 , \tag{13}$$

which, like the MKDV equation, is soluble by the inverse scattering method and has envelope solitons. Making the same transformation on the MKDV equation gives the Hirota equation[7] which also reduces to the NLS equation in the limit of large k_0.

III. CONSTANTS OF THE MOTION

The conserved quantities for a nonlinear evolution equation are closely related to the existence of an inverse scattering transform for the equation. In particular, all the equations soluble by the inverse scattering method (e.g. the MKDV equation) have an infinite number of conserved quantities. For the CMKDV equation we have only been able to find four constants of the motion, indicating that the equation is not soluble by inverse scattering.

In writing down these constants of the motion we assume that v and all its derivatives converge to 0 sufficiently rapidly as $|\xi| \to \infty$ that all the integrals we give here are convergent.

The simplest of the constants of motion is

$$I_1 = \int_{-\infty}^{\infty} v(\tau, \xi)\, d\xi = \text{const.} \tag{14}$$

This is constant since the second two terms in the CMKDV equation are a perfect derivative. The physical interpretation of (14) is that the electric field is derivable from a potential (which is the case since the waves are electrostatic). The constant is then proportional to the potential difference between $\xi = -\infty$ and $\xi = \infty$.

Other constants of the motion may be derived from the Lagrangian density for the CMKDV equation. By a straightforward generalization of the Lagrangian density for the RMKDV equation[3] we obtain

$$L = \tfrac{1}{2}(\phi_{1\xi}\overline{\phi}_{1\tau} + \overline{\phi}_{1\xi}\phi_{1\tau} + \phi_{1\xi}^2\overline{\phi}_{1\xi}^2) + \phi_{1\xi}\overline{\phi}_{2\xi} + \overline{\phi}_{1\xi}\phi_{2\xi} + \phi_2\overline{\phi}_2 \,, \tag{15}$$

where $\overline{\phi}_1 = \phi_1^*$ and $v = \phi_{1\xi}$. The conserved densities are then $-D = \phi_{i\xi}\,\partial L/\partial\phi_{i\tau} = |v|^2$ and $H = L - \phi_{i\tau}\,\partial L/\partial\phi_{i\tau} = \frac{1}{2}|v|^4 + v^* v_{\xi\xi} + v v_{\xi\xi}^* + |v_\xi|^2$. Thus we have

$$I_2 = \int_{-\infty}^{\infty} \tfrac{1}{2}|v(\tau, \xi)|^2\, d\xi = \text{const.}\,, \tag{16}$$

and

$$I_3 = \int_{-\infty}^{\infty} \tfrac{1}{2}|v(\tau, \xi)|^4 - |v_\xi(\tau, \xi)|^2\, d\xi = \text{const.}\,, \tag{17}$$

where, in deriving (17), we have integrated the middle terms in H by parts. The physical meaning of (16) is that the forces on the plasma at $\tau = \tau_1$ equal those at $\tau = \tau_2$, where the forces are given by integrating the Maxwell stress tensor, which is proportional to the square of the electric field. From (16) and (17) we can derive "Newton's first law" for the CMKDV equation, i.e. $d\overline{\xi}/d\tau = \frac{3}{2}\, I_3/I_2 = \text{const.}$, where the center of gravity, $\overline{\xi}$, is defined by

$$\overline{\xi} = \frac{\int_{-\infty}^{\infty} \xi\, \frac{1}{2}|v|^2\, d\xi}{\int_{-\infty}^{\infty} \frac{1}{2}|v|^2\, d\xi} \,. \tag{18}$$

The fourth and last constant of the motion we have found is a statement of the conservation of physical power flow, i.e. the power entering at $\tau = \tau_1$ equals that leaving at $\tau = \tau_2$, or

$$I_4 = \int_{-\infty}^{\infty} |v(\tau, k)|^2/k \, dk = \text{const.} \tag{19}$$

[Recall that the power flow is proportional to $|v(k)|^2/k$.] In (19) the principle part may be taken if the integrand is divergent at $k = 0$. In real space (19) can be written as

$$\int_{-\infty}^{\infty} (q^* q_\xi - q q_\xi^*) \, d\xi = \text{const.}, \tag{20}$$

where $v = q_\xi$. Equation (20) is true for any equation of the form

$$q_\tau + q_{\xi\xi\xi} + |G(q)|^2 q_\xi = 0, \tag{21}$$

where G is any operator. For the CMKDV equation we have $G(q) = q_\xi = v$, while for the MKDV equation we have $G(q) = q = v$. Note that (20) is convergent if $q_\xi \to 0$ as $|\xi| \to \infty$. We do not require that $q \to 0$. Thus (20) holds for the CMKDV equation even if $I_1 \neq 0$.

In a periodic system, such as is used for the numerical integration, we may replace the definition of $I_{1,2,3}$ by integrals over one period. The definition of I_4 becomes a sum over Fourier modes. However I_4 is only conserved if q (the integral of v) is also periodic, which implies that $I_1 = 0$. (This means there will be no $k = 0$ contribution to the Fourier sum.)

IV. NUMERICAL RESULTS

In order to understand the behavior of the CMKDV equation we examine the solutions numerically for initial conditions,

$$v(\tau = 0, \xi) = A \,\text{sech}(\xi) \exp(ik_0 \xi). \tag{22}$$

(Recall that τ, although treated as a time-like coordinate is really a spatial coordinate. Thus the "initial" conditions are in fact the boundary conditions at some constant x surface in the plasma.) Taking the width of the envelope in (22) to be unity is not a restriction since we can use (5) to extend our results to cover any width of the initial envelope.

The numerical integration is carried out in Fourier space. The representation in real space is used only for computing the nonlinear term in the CMKDV equation and for displaying the results. The parameters used in the numerical integration which are shown in the figure captions are: n, the number of grid points in ξ; $\delta\tau$ the stepsize in τ; L, the length of the system in ξ (periodic boundary conditions are used). Only the $n/2$ lowest Fourier modes are retained in order to prevent aliasing when computing the nonlinear term.

To gauge the accuracy of the integration, we check how well the constants of motion are conserved. I_1 is automatically conserved by the numerical scheme. I_4 is not conserved for these initial conditions since the system is periodic in ξ and $I_1 \neq 0$. So we give just δ_2 and δ_3, where $\delta_2 = |I_2(\tau) - I_0(0)|/I_2(0)$ and $\delta_3 = |I_3(\tau) - I_3(0)|/\hat{I}_3(0)$ where the definition of $\hat{I}_3$ is the same as that of I_3 (17) except that it has a plus sign instead of a minus sign.

Figure 1 shows the evolution for $A = 3$, $k_0 = 1$. The bulk of the energy ends up in two constant phase solitary pulses which travel to the right. (Note that the real and imaginary parts of v are proportional to one another.) These constant phase pulses have also been found by Kuehl.[8]

In Fig. 2 we show the evolution for $A = 5$, $k_0 = 3$. In this case most of the energy ends up in two envelope solitary pulses, the taller one having a small positive velocity and the shorter one a negative velocity. In the next sections we will examine the behavior of these two types of solitary pulses in greater detail.

V. CONSTANT PHASE PULSES

Since for the constant phase pulses θ_ξ is 0, (9) reduces to the MKDV equation with $\kappa = 3$. For this equation the solitary pulses are solitons, whose general form is given by (A13). Of these the class for which $\theta_\xi = 0$ is exact are those with $k = 0$ so that the general form of the constant phase pulses is

$$v = \sqrt{2}\, a \operatorname{sech}[a(\xi - \xi_0 - a^2\tau)]\exp(i\theta_0)\,. \tag{23}$$

These constant phase pulses do not behave as solitons in the CMKDV equation. The reason for this is that if we collide two such pulses with different values of the phase, θ_0, then θ_ξ will be nonzero during the collision. Figure 3 shows the results of such a collision. After the collision the phases of the pulses have changed, their heights have changed and some radiation is produced. ("Radiation" is used in the sense of inverse scattering theory to mean that part of the solution which is not associated with the solitary waves.) For comparison we have also shown the same collision in the MKDV equation (with $\kappa = 3$); here the pulses (solitons in this case) have passed through one another with no change in their height or phase.

The collision in the CMKDV equation results in the phases of the pulses being approximately interchanged. This is shown in more detail in Fig. 4, where we have plotted the final phases of the pulses as a function of the initial difference in phases, $\Delta\theta$. The ratio of initial heights is 2, the same as in Fig. 3. The approximate phase interchange occurs for collisions with $\Delta\theta \lesssim \frac{3}{4}\pi$.

We also measured the velocities of the pulses after collisons as a function of the initial phase difference, $\Delta\theta$, and again with the initial ratio of height being 2 (initial ratio of velocities = 4). We find the faster (i.e. taller) pulse always speeds up, while the slower one slows down. The sum of the final velocities is approximately the same as the sum of the initial velocities (to within 5%). No change in the velocities occurs for $\Delta\theta = 0$ and π (as expected since the CMKDV equation reduces to the MKDV equation in these cases). The maximum change in the velocities occurs for $\Delta\theta = 0.8\pi$, for which the fast pulse speeds up by 18%, while the slow pulse becomes lost in the radiation (this is due to the fact that we integrate the equation with periodic boundary conditions so the radiation never dies away). For $\Delta\theta < \frac{1}{4}\pi$, the changes in the velocities are small, less than 1% of the initial velocity of the faster pulse.

VI. ENVELOPE PULSES

In this section we examine the envelope pulses observed in Fig. 2 in more detail. We let the pulses have the form,

$$v(\tau, \xi) = V(\zeta) \exp[i(k_0 \xi - \omega_0 \tau)], \tag{24}$$

where $\zeta = \xi - c\tau$ and k_0, ω_0 and c are real, but V is *complex*. This form allows a phase variation with phase velocity, ω_0/k_0, different from c, but requires that any local features in the phase of v travel at the pulse velocity, c.

Since, by assumption, V forms a pulse, we have $V(|\zeta| \to \infty) \to 0$. In this limit the nonlinear term in the CMKDV equation may be neglected. Supposing that $V(\zeta \to -\infty) \sim \exp(a\zeta)$, where a is real and positive, we find that $V(\zeta \to \infty) \sim \exp(-a\zeta)$. The frequency and velocity of the pulse may then be found in terms of k_0 and a,

$$\omega_0 = k_0(3a^2 - k_0^2)\,,\ c = a^2 - 3k_0^2\,. \tag{25}$$

Substituting (24) into the CMKDV equation then gives

$$(V_{\zeta\zeta} + |V|^2V - a^2V)_\zeta + ik_0(3V_{\zeta\zeta} + |V|^2V - 3a^2V) = 0\,. \tag{26}$$

Two limits of this equation are easily treated. If $k_0 = 0$ then $V = \sqrt{2}\,a\ \mathrm{sech}(a\zeta)$. This gives the constant phase pulse (23) we studied in Sec. V. If $k_0 \to \infty$, then $V = \sqrt{6}\,a\ \mathrm{sech}(a\zeta)$ or

$$v = \sqrt{6}\,a\ \mathrm{sech}\{a[\xi - (a^2 - 3k_0^2)\tau]\}\exp\{i[k_0\xi - k_0(3a^2 - k_0^2)\tau]\}\,. \tag{27}$$

[In both these cases we have omitted a possible shift of the ξ origin and a phase factor $\exp(i\theta_0)$.] Equation (27) is identical to the soliton solution for the MKDV equation (A13). If we compare (27) with the soliton of the NLS equation (13), $u = a\ \mathrm{sech}(a\zeta)\exp(-ia^2\eta)$ or undoing the transformation that gave (12)

$$v = \sqrt{6}\,a\ \mathrm{sech}[a(\xi + 3k_0^2\tau)]\exp\{i[k_0\xi - k_0(3a^2 - k_0^2)\tau]\}\,, \tag{28}$$

we see that there is a difference of a^2 in the pulse velocities.

Away from the limits $k_0 = 0$ and $k_0 \to \infty$, we can perform perturbation analyses on (26). For small k_0 we may attempt to develop a series expansion for V in k_0. Without loss of generality we take $a = 1$ [this may be achieved by use of the scaling invariance of the CMKDV equation (5)]. Expanding V as $V_0 + V_1 + \ldots$, with $V_n = O(k_0^n)$ and $V_0 = \sqrt{2}\ \mathrm{sech}(\zeta)$, we find

$$V_{1\zeta\zeta} + |V_1|^2V_1 - V_1 = 4\sqrt{2}\,ik_0\int^\zeta \mathrm{sech}^3(\zeta)\,d\zeta \equiv C(\zeta)\,. \tag{29}$$

Now $C(\infty) - C(-\infty) = 2\sqrt{2}\pi ik_0$, so that either $C(\infty)$ or $C(-\infty)$ or both are nonzero (for $k_0 \neq 0$). Supposing $C(\infty)$ to be nonzero and assuming $V_1 \to 0$ as $\zeta \to \infty$, we may write $V_{1\zeta\zeta} - V_1 = C(\infty)$ for ζ sufficiently large. But this gives $V_1 \to -C(\infty)$ as $\zeta \to \infty$. Thus V_1 must be nonzero at either $\pm\infty$, and so V cannot form a pulse for small (but finite) k_0.

For large k_0 we develop an asymptotic series for V in $\varepsilon \equiv a/k_0$. Although (26) is an irregular perturbation problem (for $\varepsilon \to 0$), we are only interested in the regular solutions which are close to the solution for $\varepsilon = 0$. Thus we write (26) as

$$(3V_{\zeta\zeta} + |V|^2V - 3a^2V)_n = i\varepsilon a^{-1}[(V_{\zeta\zeta} + |V|^2V - a^2V)_\zeta]_{n-1}\,. \tag{30}$$

where subscripts n and $n-1$ denote the orders of the terms, and $V = V_0 + V_1 + V_2 + \ldots$, with $V_n = O(\varepsilon^n)$ and $V_0 = \sqrt{6}\, a\, \mathrm{sech}(a\zeta)$. We then find that

$$V = \sqrt{6}\, a\, \mathrm{sech}(a\zeta)\{1 + i\varepsilon \tanh(a\zeta) + \tfrac{1}{3}\varepsilon^2[\tanh^2(a\zeta) - \tfrac{1}{2}] + iO(\varepsilon^3) + O(\varepsilon^4)\}\,. \tag{31}$$

From this we obtain

$$|V| = \sqrt{6}\, a\, \mathrm{sech}(a\zeta)\{1 + \tfrac{1}{6}\varepsilon^2[5\tanh^2(a\zeta) - 1] + O(\varepsilon^4)\}\,, \tag{32}$$

$$\arg(V) = \varepsilon \tanh(a\zeta) + O(\varepsilon^3)\,, \tag{33}$$

and

$$\int_{-\infty}^{\infty} |V|\, d\zeta = \sqrt{6}\,\pi[1 + \tfrac{1}{4}\varepsilon^2 + O(\varepsilon^4)]\,. \tag{34}$$

For finite k_0 we resort to numerically integrating (26). For $0 < |k_0/a| \lesssim 0.5$ no pulse is formed. For other values of k_0 a pulse is obtained. Fig. 5 shows the result for $k_0/a = 0.5$ and 2. For $k_0/a = 0.5$, the pulse does not come back down to zero very well. Nevertheless we have integrated the CMKDV equation with this pulse (cutoff at its minimum) as an initial condition and we find that it is indeed stationary for a long time (at least till $a^3\tau \sim 50$). If a pulse is formed then from the symmetries of (26) it has the property, $V(-\zeta) = V^*(\zeta)$ [with appropriate choice of origin and on multiplication by an appropriate constant, $\exp(i\theta_0)$]. Also shown in Fig. 5(c and d) is the asymptotic pulse shape for $\varepsilon = \frac{1}{2}$ as given by (32) and (33). The agreement between this and the pulse obtained numerically is quite good. In Fig. 6 we plot the pulse area, $\int_{-\infty}^{\infty} |V|\, d\zeta$, comparing the analytical (34) and numerical results. Again the agreement is quite good for $k_0/a \gtrsim 2$. Note that the area for small k_0 is considerably larger than the area for the constant phase pulses ($k_0 = 0$).

VII. EVOLUTION OF A PULSE

We are now in a position to have some analytic understanding of the evolution of a pulse of the form considered in Sec. IV (22). There are two properties of the CMKDV equation that distinguish it from the MKDV equation. Firstly as we saw in Sec. II the relative strength of the nonlinear term is different in the limits of slow and rapid phase variation. Thus the solitary waves in these two limits have different areas. The other distinguishing property is that, unlike the MKDV equation, there is not a continuous transition between the constant phase pulses and the envelope pulses. (In the MKDV equation the limit $k_0 \to 0$ gives the constant phase pulses.) Thus it is of interest to determine how the CMKDV equation does make the transition from one type of pulse to the other.

Let us begin by considering the limit where k_0 is large, but A is finite. In this limit the equation approximately reduces to the MKDV equation (with $\kappa = 1$), and so the solution is given by the inverse scattering method (see Appendix). The initial pulse breaks up into N solitons where $A/\sqrt{6} = N + \varepsilon, -\frac{1}{2} < \varepsilon \leq \frac{1}{2}$. In the appendix we identify the two "time" scales on which the pulse evolves, a self-focussing time scale, τ_s, the time required for the relative phases of two solitons to change by π and a filamentation time scale, τ_f, the time for two solitons to pass through each other. (Again remember that τ, although treated like time, is in fact a spatial coordinate.) Using (A37) and (A38) we obtain $\tau_s = \frac{2}{3}\pi/(k_0 A^2) \ll \tau_f = 3\sqrt{6}A^{-3}$. The approximation of the CMKDV equation by the NLS equation only describes phenomena on the former (very short) time scale [in (13) $\eta = 3k_0\tau$], and so does not predict filamentation for these initial conditions [see (27) and (28)].

Suppose we keep k_0 large but allow A to be comparable to k_0. Since the initial pulse has a smooth envelope variation, its early evolution is described by the MKDV equation. The tallest soliton present in the initial pulse has an inverse width $a_N \approx 2A/\sqrt{6}$ (for $A \gg 1$). Thus the most rapid variation of the envelope will be over a distance of a_N^{-1}. However, since A is $O(k_0)$, a_N is $O(k_0)$ and the assumption that the envelope of v is slowly varying compared with the phase is false at some later time, when the tallest soliton emerges. We expect the MKDV solitons to turn into the envelope pulses with finite a/k_0 that were studied in the previous section. Taking a for the envelope pulses to be the same as the inverse widths a_j given by the inverse scattering method, we see that when $A \gtrsim \sqrt{6}k_0$ the tallest envelope pulse would have $k_0/a < 0.5$. However we saw in Sec. VI that there are no envelope pulses in this range of k_0/a. Furthermore the envelope pulse with $k_0/a = 0.5$ has an envelope area which is more than twice the area of a constant phase pulse (see Fig. 6). This suggests that, if A is increased, the tallest envelope pulse should break up into two or three constant phase pulses. In Fig. 7 we see this happening. Recall that for $A = 5$, $k_0 = 3$ we obtained two envelope pulses (Fig. 2). Here (Fig. 7) A has been increased by 1 to 6. Now the tallest of the envelope pulses breaks up into three constant phase pulses. From this we determine that a more accurate condition for the appearance of constant phase pulses is $A \gtrsim 2k_0$. Put another way, the break-up into constant phase pulses occurs when the equation sees sufficent area over a distance where the phase is roughly constant.

With A sufficiently large only constant phase pulses appear. We studied the interaction of these pulses in Sec. V. If $A \gg k_0$ the phases of neighboring pulses are close together. Thus the initial evolution is governed by the MKDV equation with $\kappa = 3$. The effect of the finite θ_ξ in (9) is to cause the phases of the pulses to be interchanged on collision (see Fig. 4). This ensures that only small angle collisions take place subsequently, and the overall features of the solution are approximately given by the MKDV equation. In particular the time scale for filamentation is given by $\tau_f = \sqrt{2}A^{-3}$. Self-focussing does not take place with constant phase pulses.

Figure 8 shows schematically how the initial conditions (22) break up into solitary pulses. For k_0 small there are N constant phase pulses where $N - \frac{1}{2} < A/\sqrt{2} < N + \frac{1}{2}$. For k_0 large there are N envelope pulses where $N - \frac{1}{2} < A/\sqrt{6} < N + \frac{1}{2}$. The transition from having all envelope pulses to all constant phase pulses occurs in a wedge shaped region as shown. For the MKDV equation this figure would just consist of horizontal lines at $A(\kappa/6)^{1/2} = N - \frac{1}{2}$.

We expect Fig. 8 to qualitatively apply to more general initial conditions. If the initial conditions are the product of an envelope, $|v|$, which has a single maximum, and a phase factor with an approximately linearly increasing phase, then A, the vertical axis in Fig. 8, would be regarded as some measure of the area of $|v|$, whereas k_0, the horizontal axis, would give a measure of the number of wavelengths over the width of $|v|$.

As an example consider the excitation of lower hybrid waves by an array of M waveguides phased $0, \pi, 0, \pi, \ldots$ Take the total width of the array to be $\Delta\xi$ and the normalized field to be a constant, v_0. Then k_0 corresponds to M and A corresponds to $v_0 \Delta\xi/\pi$. We obtain constant phase pulses if ($A \gtrsim \frac{1}{2}\sqrt{2}$)

$$v_0 \Delta\xi \gtrsim \tfrac{1}{2}\sqrt{2}\pi \,, \tag{35}$$

and ($A \gtrsim 2k_0$)

$$v_0 \Delta\xi/M \gtrsim 2\pi \,. \tag{36}$$

If this last condition is not met we obtain envelope pulses if ($A \gtrsim \frac{1}{2}\sqrt{6}$)

$$v_0 \Delta\xi \gtrsim \tfrac{1}{2}\sqrt{6}\pi \,. \tag{37}$$

To estimate the time scales of the evolution of this initial condition we use (A37) and (A38) with B

$= v_0/\sqrt{2}$ for constant phase pulses and $v_0/\sqrt{6}$ for envelope pulses and with $k_0 = \pi M/\Delta\xi$. Thus the filamentation time for constant phase pulses is

$$\tau_f = \sqrt{2} v_0^{-3} . \tag{38}$$

The filamentation time for envelope pulses is greater by a factor of $3^{3/2}$, while the self-modulation time for these pulses is

$$\tau_s = \tfrac{2}{3}\Delta\xi/(M v_0^2) . \tag{39}$$

VIII. THE BOUNDARY VALUE PROBLEM

Up till now we have been regarding τ as a time-like coordinate, and we have been solving the CMKDV equation as an initial value problem [with $v(\tau = 0, \xi)$ imposed]. However τ is in fact a spatial coordinate, proportional to x, the distance into the plasma. Thus we should really solve the CMKDV equation as a boundary value problem in a slab $0 < \tau < \tau_1$. The boundary value problem would be equivalent to the initial value problem if we could be sure that all the components of v travel in the $+\tau$ direction. Let us examine this possibility. The direction of propagation of a wave may be defined in terms of its power flow which in this case is $|v(k)|^2/k$. Thus only the positive k components travel in the $+\tau$ direction and so the initial value problem is physically correct only if there are no negative k components to v. However if we begin at $\tau = 0$ with no negative k components [i.e. with v satisfying (11)], the equation, being nonlinear, will generate negative k components at finite τ. This is easy to see in the case where the initial amplitude is large enough to give constant phase pulses (see Fig. 8), since these pulses have equal positive and negative power flows. Therefore when treating the physical problem we should solve the CMKDV equation as a boundary value problem. To be more precise we should only impose the incident wave at $\tau = 0$, $v(\tau = 0, k > 0)$. At the far boundary of the plasma, $\tau = \tau_1$, we specify a radiation condition that there is no reflected wave, $v(\tau_1, k < 0) = 0$. We shall try to find the transmitted wave at τ_1, $v(\tau_1, k > 0)$ and the reflected wave at $\tau = 0$, $v(0, k < 0)$. (Even if there were a metallic boundary at $\tau = \tau_1$ we would still impose a radiation condition. The reflection caused by a metal wall converts the wave to the other resonance cone, while the CMKDV equation describes the waves in a single resonance cone only. The reflection caused by the nonlinearity causes both k_x and k_z to change signs so that the reflected wave is still in the original resonance cone.)

We do not know whether this boundary value problem is well posed. However we have attempted its numerical solution. We define the positive and negative power flows,

$$P_{\pm}(\tau) = \int_0^{\pm\infty} |v(\tau, k)|^2/k \, dk \,. \tag{40}$$

We first pick $v(\tau = 0, k < 0)$ (we will describe how in a moment) and some small convergence parameter, ε. An iteration is then performed with the following steps: impose $v(0, k > 0)$; integrate the equation to $\tau = \tau_l$; if $P_-(\tau_l) \le \varepsilon P_+(\tau_l)$, stop the iteration; set $v(\tau_l, k < 0) = 0$; integrate the CMKDV equation backwards to $\tau = 0$; go to the beginning of the iteration. We perform this procedure beginning at $\tau_l = 0$ with $v(0, k < 0) = 0$, and increasing τ_l by $\delta\tau$ after the convergence criterion is met. We use $v(\tau = 0, k < 0)$ for $\tau_l = \tau_l - \delta\tau$ as the initial guess for $v(\tau = 0, k < 0)$ for $\tau_l = \tau_l$.

When solving the boundary value problem in this way, we choose

$$v(\tau = 0, k > 0) = A\pi\, u(k - k_0)(k - k_0)\exp[-(k - k_0)^2/4] \,, \tag{41}$$

where $k_0 \ge 0$. In real space we have

$$v(\tau = 0, \xi)|_{k > 0} = A[1 + \xi Z(\xi)]\exp(ik_0\xi) \,, \tag{42}$$

where Z is the plasma dispersion function. [Z is defined, for real ξ, by (11) where $w(\xi) = 2\sqrt{\pi}\, i \exp(-\xi^2)$.] We define the reflectivity, R, by

$$R = P_-(0)/P_+(0) \,. \tag{43}$$

Figure 9 shows R as a function of the system width, τ_l, for various A and k_0. The largest reflectivity occurs when solving the CMKDV equation as an initial value problem would have given constant phase pulses ($A = 3$, 4 and $k_0 = 0$). The values of τ_l at which the reflection first becomes appreciable in these two cases are given by the filamentation time (38). The oscillations in R for $A = 4$ and $k_0 = 1$ suggest the presence of some sort of interference.

The crosses in the plots for $A = 4$ and $k_0 = 0, 1$ show where our numerical procedure ceased to converge. There are two possible explanations for this. Firstly it may be that an answer exists but that the numerical procedure does not find it. The second possibility is that there is no answer, i.e. the CMKDV equation as a boundary value problem is ill-posed. In this case the most likely explanation is that the steady-state assumption, under which the CMKDV equation was derived, is false. In other words, even though the source at $\tau = 0$ is at a constant frequency and is on for an infinitely long time the field in the plasma never reaches a steady state.

IX. DISCUSSION

We pursue the example introduced in Sec. VII, but now we give the results in more convenient terms in order to apply them to lower hybrid heating. At whatever position in the plasma we take to be the x origin we impose

$$\tilde{E}_x(x = 0, z) = E_{x0}\exp(i\pi z/\delta z)\,u(z + \tfrac{1}{2}\Delta z)\,u(-z + \tfrac{1}{2}\Delta z)\,, \tag{44}$$

where $\Delta z = M\,\delta z$. This models the excitation by M alternately phased waveguides each with width δz, the total width of the array being Δz. For simplicity we take $T_i \ll T_e$, $\omega_{pe}^2 \ll \Omega_e^2$. We then have $\xi = (x - gz)/(\sqrt{3}\lambda_{De})$, $\tau = x/(2\sqrt{3}\lambda_{De})$, $v = \tilde{E}_x^*/(4n_0T_e/\epsilon_0)^{1/2}$. We define the following quantities: $\Delta x = g\Delta z$, the width of the lower hybrid ray in the x direction; $E_{z0} = gE_{x0}$, the parallel electric field at $x = 0$; $\alpha = E_{z0}\,\delta z/T_e$, the ratio of the potential across a single waveguide to the electron temperature; $\beta = \frac{1}{4}\epsilon_0 E_{x0}^2/(n_0T_e)$, the ratio of the electric to plasma energy densities. The conditions under which constant phase pulses are predicted for the inital value problem are, from (35) and (36),

$$M\alpha \gtrsim \sqrt{6}\pi\,, \quad \alpha \gtrsim 4\sqrt{3}\pi\,. \tag{45}$$

The condition for envelope pulses is (37)

$$M\alpha \gtrsim 3\sqrt{2}\pi\,. \tag{46}$$

The filamentation scale distance for constant phase pulses is [see (38)]

$$x_f \approx 4\sqrt{6}(T_e/E_{x0})\beta^{-1}\,. \tag{47}$$

The self-focussing distance for envelope pulses is [see (39)]

$$x_s \approx \tfrac{4}{3}\Delta x/(M\beta)\,. \tag{48}$$

We showed in Sec. VIII that it is incorrect to solve the problem as an initial value problem.

However the results of the inital value problem will only differ greatly from those of the correct boundary value problem if the reflection is appreciable. For this to be so we need that the constant phase pulses be predicted by the initial value problem (45) and that the thickness of the plasma, x_1, exceed the filamentation distance, x_f (47).

We illustrate these results with two examples. Take $n_0 = 10^{13}\ \mathrm{cm}^{-3}$, $T_e = 1$ keV, $E_{x0} = 10$ kV/cm, $\delta z = 2.5$ cm, $M = 4$, $g = \frac{1}{10}$. This is representative of the central plasma conditions and fields for lower hybrid heating in present-day tokamaks. We then have $\Delta z = 10$ cm, $\Delta x = 2.5$ mm, $E_{z0} = 250$ V/cm, $\alpha = 0.625$, $M\alpha = 2.5$, $\beta = 1.4 \times 10^{-3}$. Thus pulses of neither sort are formed. The ponderomotive force does not have a strong effect on the propagation.

As a second example consider $n_0 = 5 \times 10^{11}\ \mathrm{cm}^{-3}$, $T_e = 25$ eV, $E_{x0} = 4$ kV/cm, $\delta z = 2.5$ cm, $M = 4$, $g = \frac{1}{10}$. This could represent the plasma conditions close to the edge of a present-day tokamak or conditions encountered in a smaller laboratory-scale experiment. In this case we have $\Delta z = 10$ cm, $\Delta x = 1$ cm, $E_{z0} = 400$ V/cm, $\alpha = 40$, $M\alpha = 160$, $\beta = 0.18$. Now the conditions for constant phase pulses, (45), are satisfied, and that $x_f = 4$ mm. If we are considering the propagation of lower hybrid waves through the inhomogeneous outer region of the plasma then, provided the gradient scale length exceeds x_f, we expect strong nonlinear reflection to occur.

Let us review the assumptions made in deriving the CMKDV equation, and see how they effect this conclusion. The first of the assumptions is that the plasma is homogeneous. However, the region of interest in a tokamak is close to the edge where the plasma is inhomogeneous. A simple estimate of the validity of the assumption of homogeneity is that the gradient scale length exceeds the filamentation length (which is also one of the conditions for reflections to be important). Analytic studies of the nonlinear propagation of lower hybrid waves in an inhomogeneous plasma as described by the NLS equation (with an additional term describing the inhomogeneity) have been carried out by Leclert *et al.*[9] They find an increase in the soliton threshold from the homogeneous result. Numerical work has been carried out on the CMKDV equation with inhomogeneity by Sanuki and Ogino.[10] However, they do not recognise the phenomenon of nonlinear reflection. More work on this aspect of the problem is required.

The second assumption is that the system is two-dimensional. The addition of a third dimension to the NLS equation describing lower hybrid wave propagation rendered the solitons unstable.[11,12] Inclusion of the third dimension, y, to lowest order in the CMKDV equation gives the complex modified Kadomstev-Petviashvili equation,

$$v_\tau + \int^\xi v_{\eta\eta}\, d\xi + v_{\xi\xi\xi} + (|v|^2 v)_\xi = 0\,, \tag{49}$$

where $\eta = \lambda^{-2}\eta'$ and $\eta' = y/(K_\perp^{1/2}\Delta)$ [cf. (2) - (5)]. However we do not expect the third dimension to be important in our case since the interaction length in x, x_f, is so much smaller than the typical y dimension (~ 10 cm).

The final assumption is that the system is in steady state. We suggested that perhaps this assumption is false for the CMKDV equation as a boundary value problem. However nonlinear reflection will probably still occur, even though the plasma does not reach a steady state. A similar result was obtained by Morales[13] who considered the nonlinear coupling of waves to the plasma edge. In this case steady state was not achieved. (The nonlinear reflection discussed by Morales[13] has a different physical origin from that discussed here. In his work the reflection was due to the waves changing the position of the cutoff where $\omega = \omega_{pe}$. Our reflection is due to scattering off the ponderomotive density fluctuations and so could not occur in his system which allowed no z modulation of the field.) If we allow the electric field to have a slow time dependence [multipying the $\exp(-i\omega t)$ dependence already included] then to lowest order we obtain a two-dimensional generalization of the NLS equation,

$$iv_\sigma + \int^\xi v_\tau\, d\xi + v_{\xi\xi} + |v|^2 v = 0\,, \tag{50}$$

where $\sigma = \lambda^{-2}\sigma'$ and $\sigma' = t/[K_\parallel \partial(K_\perp/K_\parallel)/\partial\omega]$.

In summary, we have studied the propagation of lower hybrid waves as described by the CMKDV equation. When treated as an initial value problem in x, two types of solitary waves are found, one which has a constant phase, while the other is an envelope pulse. These pulses are not solitons. There is not a continuous transition from one type to the other. When constant phase pulses are produced, it means that reflection is occurring and the problem should be solved as a boundary value problem. Applying these results to RF heating of a tokamak we find that the effect of the ponderomotive force can be to cause strong reflection of the lower hybrid waves close to the edge of a tokamak type plasma. Before a definitive answer can be given as to the magnitude of this effect the problem needs to be examined further allowing for the effects of inhomogeneity and a time dependence for the fields.

ACKNOWLEGDEMENTS

We wish to thank J. D. Meiss and N. R. Pereira for making available their program for solving nonlinear evolution equations. One of us (FYFC) would like to thank the members of the Theoretical Physics Group of Lawrence Berkeley Laboratory for their hospitality.

This work was supported by U.S. Department of Energy under Contracts EY-76-C-02-3073 and EG-77-G-01-4107, the National Science Foundation under Grant ENG 77-00340, and the U.S. Air Force under Grant AFOSR 77-3321.

APPENDIX. INVERSE SCATTERING METHOD FOR THE MKDV EQUATION

In this appendix we briefly review the solution of the MKDV equation (8) by the inverse scattering method. We will find it convenient to rescale v, by $v = (6/\kappa)^{1/2} q$, so that the MKDV equation reads,

$$q_\tau + q_{\xi\xi\xi} + 6|q|^2 q_\xi = 0 . \tag{A 1}$$

In the course of outlining the solution for the MKDV equation, we will point out the modifications necessary for obtaining solutions to the NLS equation,

$$q_\tau + iq_{\xi\xi} + 2i|q|^2 q = 0 . \tag{A 2}$$

1. Direct Scattering Problem

The MKDV equation is one of the class of equations covered by the methods of Ablowitz *et al.*[4] The scattering problem is the same as that for the NLS equation, which was introduced by Zakharov and Shabat,[14]

$$\psi_{1\xi} + i\lambda\psi_1 = q\psi_2 , \tag{A 3}$$

$$\psi_{2\xi} - i\lambda\psi_2 = q^*\psi_1 . \tag{A 4}$$

These equations will be recognized as those for a backward wave oscillator. It will be assumed that $q \to 0$ as $|\xi| \to \infty$. Equations (A 3) and (A4) are solved for $q = q(\tau = 0, \xi)$ and with boundary conditions

$$\psi_1 \to \exp(-i\lambda\xi) , \ \psi_2 \to 0 , \ \text{for } \xi \to -\infty . \tag{A 5}$$

Solving (A 3) and (A 4) gives

$$\psi_1 \to \alpha(\lambda) \exp(-i\lambda\xi) , \ \psi_2 \to \beta(\lambda) \exp(i\lambda\xi) , \ \text{for } \xi \to \infty . \tag{A6}$$

The complete scattering data, from which q may be reconstructed, consists of the incident and reflected wave amplitudes, $\alpha(\lambda)$ and $\beta(\lambda)$, for λ real, and the residues, $\mu_j = \beta(\lambda_j)/[\partial\alpha(\lambda)/\partial\lambda]_{\lambda_j}$, for all $\lambda = \lambda_j$ such that $\alpha(\lambda_j) = 0$ and $\mathrm{Im}(\lambda_j) > 0$. The data for λ real gives the "radiation" part of the solution, while the data at the discrete eigenvalues, λ_j, gives the soliton part. When determining the discrete scattering data numerically, the following relation is useful for determining the residues, μ_j:[15]

$$[\partial\alpha(\lambda)/\partial\lambda]_{\lambda_j} = -[2i/\beta(\lambda_j)]\int_{-\infty}^{\infty}\psi_1\psi_2\,d\xi\,. \tag{A 7}$$

[Note that $\psi_{1,2}(|\xi|\to\infty)\to 0$, for $\lambda=\lambda_j$.]

In what follows we shall neglect the radiation. This is equivalent to setting $\beta(\lambda)=0$ for real λ. We can determine the error in doing this, by comparing $\int_{-\infty}^{\infty}\frac{1}{2}|q|^2 d\xi$ for the initial conditions and for the solitons. In the case where $\beta(\lambda)=0$ for real λ, $\alpha(\lambda)$ is given by[14]

$$\alpha(\lambda)=\Pi_j(\lambda-\lambda_j)/(\lambda-\lambda_j^*)\,, \tag{A8}$$

where the product is over all the discrete eigenvalues.

The time evolution of q is reflected in the time evolution of μ_j (λ_j is independent of time). From Ref. 4 we have

$$\mu_j(\tau)=\mu_j(\tau=0)\exp(i\Omega_j\tau)\,, \tag{A9}$$

where $\Omega_j=8\lambda_j^3$ for the MKDV equation, and $-4\lambda_j^2$ for the NLS equation.

2. The N-Soliton Solution

Assuming that there are N roots of $\alpha(\lambda)$ in the upper half λ plane, and that the radiation may be neglected, the solution for both the MKDV and NLS equations then reads

$$q=-2P_jH_{jk}M_k\,, \tag{A 10}$$

where

$$P_j=\exp(-i\lambda_j^*\xi)\,,\quad M_j=i\mu_j^*(\tau)P_j\,, \tag{A 11}$$

$$\mathbf{H}=[\mathbf{I}+\mathbf{G}^*\cdot\mathbf{G}]^{-1}\,,\quad G_{jk}=\mu_j(\tau)\exp[i(\lambda_j-\lambda_k^*)\xi]/(\lambda_j-\lambda_k^*)\,. \tag{A 12}$$

(Summation over the repeated indices from 1 to N is implied.)

If there is only one discrete eigenvalue λ_j, we obtain the one soliton solution,

$$q = a_j \operatorname{sech}[a_j(\xi - \xi_j - c_j\tau)] \exp[i(k_j\xi - \omega_j\tau + \theta_j)] , \tag{A 13}$$

where

$$2\lambda_j = -k_j + ia_j , \quad \omega_j = \mathrm{Re}(\Omega_j) , \quad c_j = -\mathrm{Im}(\Omega_j)/a_j , \tag{A 14}$$

$$a_j\xi_j = \log[|\mu_j(0)|/a_j] , \quad \theta_j = -\arg[\mu_j(0)] - \tfrac{1}{2}\pi . \tag{A 15}$$

(Here a_j and k_j are real.) Thus for the MKDV equation we have

$$\omega_j = k_j(3a_j^2 - k_j^2) , \quad c_j = a_j^2 - 3k_j^2 , \tag{A 16}$$

while for the NLS equation we have

$$\omega_j = a_j^2 - k_j^2 , \quad c_j = -2k_j . \tag{A 17}$$

In the case where there are several solitons, as long as their velocities, c_j, are all *different*, the solitons will eventually all separate, and the asymptotic solution for $|\tau| \to \infty$ will be the (algebraic) sum of the individual solitons. The only effect on a given soliton of the additional solitons at $|\tau| \to \infty$ is to alter the position and phase of that soliton. If we order the eigenvalues such that $c_j < c_{j+1}$ for $0 \le j < N$, then for $\tau \to \pm\infty$ (A 15) becomes[14]

$$a_j\xi_j = \log\left(\frac{|\mu_j(0)|}{a_j}\right) + 2\sum_{p \gtrless j} \log\left|\frac{\lambda_j - \lambda_p}{\lambda_j - \lambda_p^*}\right| , \tag{A 18}$$

$$\theta_j = -\arg[\mu_j(0)] - \frac{\pi}{2} - 2\sum_{p \gtrless j} \arg\left(\frac{\lambda_j - \lambda_p}{\lambda_j - \lambda_p^*}\right) . \tag{A 19}$$

If some of the solitons have the same velocity, then they form a coupled soliton solution called a breather. For the NLS equation this happens when two or more solitons have eigenvalues with the same real part. For the MKDV equation the simplest breather solution consists of two solitons with eigenvalues satisfying $\lambda_2 = -\lambda_1^*$.[15] The transition between a two-soliton breather and the two uncoupled solitons occurs when two eigenvalues coalesce. In this case the *N-soliton solution is no longer valid since μ is divergent.* However it is possible to find the solution in this case by taking the limit as two eigenvalues come together. If we substitute

$$2\lambda_{1,2} = ia - k \pm \varepsilon , \quad \mu_{1,2}(0) = -ia \pm a^2/\varepsilon , \tag{A20}$$

into (A 10) *and then take the limit* $\varepsilon \to 0$, we obtain for the MKDV equation

$$v = 2a \, \frac{1 - 6ika^2\tau - a(\zeta - 2a^2\tau)\tanh(a\zeta)}{\cosh(a\zeta) + [a^2(\zeta - 2a^2\tau)^2 + (6ka^2\tau)^2]\,\mathrm{sech}(a\zeta)} \exp[i(k\xi - \omega\tau)]\,, \tag{A21}$$

where $\zeta = \xi - c\tau$, and c and ω are given by (A 16). For $\tau \to \infty$, (A21) becomes

$$v \to -\exp[i(k\xi - \omega\tau)]\, \Sigma_{\pm} \pm \exp[\pm i \tan^{-1}(3k/a)]\, a\, \mathrm{sech}\{a\zeta \pm \log[4a^2(9k^2 + a^2)^{1/2}\tau]\}\,. \tag{A22}$$

This consists of two equal solitons moving apart with relative velocity $2/(a\tau)$.

3. Properties of the Zakharov-Shabat Eigenvalue Problem

There are no discrete eigenvalues if[4]

$$\int_{-\infty}^{\infty} |q|\, d\xi < 0.904\,, \tag{A23}$$

where $I_0(2 \times 0.904) = 2$ and I_0 is a modified Bessel function.

All eigenvalues must satisfy

$$\mathrm{Im}(\lambda) < \max(|q|)\,. \tag{A24}$$

This states that the tallest soliton will be less than twice the maximum height of the initial pulse. We give the proof of this result for the generalized Zakharov-Shabat problem considered by Ablowitz *et al.*[4] for which (A4) reads

$$\psi_{2\xi} - i\lambda\psi_2 = r\psi_1\,. \tag{A25}$$

We multiply (A3) by ψ_1^* and (A25) by $-|\rho|^2\psi_2^*$, where ρ is a complex number (independent of ξ). Adding the resulting equations, integrating them from $\xi = -\infty$ to ∞, solving for λ and taking the imaginary part gives

$$\mathrm{Im}(\lambda) = \frac{-\int_{-\infty}^{\infty} \mathrm{Re}(q\psi_1^*\psi_2 - |\rho|^2 r\psi_1\psi_2^*)\, d\xi}{\int_{-\infty}^{\infty} |\psi_1|^2 + |\rho\psi_2|^2\, d\xi}\,. \tag{A26}$$

[In deriving this we have used e.g. $\int_{-\infty}^{\infty} \mathrm{Re}(\psi_1^*\psi_{1\xi})\, d\xi = 0$.] *Working now with the numerator of* (A26) we have

$$\text{Numerator} = -\int_{-\infty}^{\infty} \mathrm{Re}\{[(q/\rho) - (\rho r)^*]\psi_1^*\rho\psi_2\}\, d\xi$$

$$\le \int_{-\infty}^{\infty} |(q/\rho) - (\rho r)^*||\psi_1||\rho\psi_2| \, d\xi$$

$$< \max[|(q/\rho) - (\rho r)^*|] \int_{-\infty}^{\infty} |\psi_1||\rho\psi_2| \, d\xi$$

$$\le \tfrac{1}{2} \max[|(q/\rho) - (\rho r)^*|] \int_{-\infty}^{\infty} |\psi_1|^2 + |\rho\psi_2|^2 \, d\xi \qquad \text{(A27)}$$

[the last inequality coming from $(|\psi_1| - |\rho\psi_2|)^2 \ge 0$]. Since ρ is arbitrary we can perform a minimization over ρ to give

$$\mathrm{Im}(\lambda) < \tfrac{1}{2} \min_\rho\{\max_\xi[|(q/\rho) - (\rho r)^*|]\} \, . \qquad \text{(A28)}$$

(Without loss of generality we may restrict ρ to the positive real numbers.) For our problem $r = -q^*$. The minimization over ρ gives $\rho = 1$, from which (A24) follows.

If $q = Q\exp[i(k_0\xi + \theta_0)]$, then the eigenvalues are the same as for $q = Q$ except that they all have real parts decreased by $\frac{1}{2}k_0$. The values of μ_j are all multiplied by $\exp(i\theta_0)$. This enables us to consider only real q (as far as solving the eigenvalue problem goes), and still be able to generalize the results to cover the case where q is the product of a real function and $\exp[i(k_0\xi + \theta_0)]$.

For q real we begin by noting[4] that either λ_j is pure imaginary, or if λ_j is complex, then there is another eigenvalue equal to $-\lambda_j^*$. (We shall call such a pair of eigenvalues a "complex pair.") Only in rather restrictive cases can statements be made as to the number and type of eigenvalues we will have. If q is antisymmetric, then the eigenvalues will always occur in complex pairs.[16] If q is non-negative, then it may be shown[16] that the condition $\int_{-\infty}^{\infty} q \, d\xi = (N - \frac{1}{2})\pi$ (N an integer) corresponds to the threshold for a soliton with $\lambda = 0$. The term "threshold" may be misleading here. A simple example will show why. Suppose $q = 1$ for $L < |\xi| < 2L$, and $q = 0$ otherwise. Let us consider what eigenvalues we have as we increase L from 0. At $L = \frac{1}{4}\pi$ we reach the threshold for a single soliton ($\lambda = 0$), in accordance with the threshold condition. At $L = 0.3126\pi$ a complex pair of eigenvalues appear ($\lambda = \pm 0.9542$). This complex pair coalesces on the imaginary axis at $L = 0.6932\pi$ and $\lambda = 0.2077i$ [see (A21)]. The first eigenvalue is then at $\lambda = 0.4641i$. The double eigenvalue then splits in two again, one eigenvalue going up the imaginary axis and the other going down. At $L = \frac{3}{4}\pi$, when $\int_{-\infty}^{\infty} q \, d\xi = \frac{3}{2}\pi$, and hence at the "threshold" for a soliton, the lowest eigenvalue *disappears* at $\lambda = 0$. However the number of eigenvalues, N, is given by

$$(N - \tfrac{1}{2})\pi < \int_{-\infty}^{\infty} q \, d\xi \le (N + \tfrac{1}{2})\pi \, , \qquad \text{(A29)}$$

if the following conditions are satisfied: q is non-negative; there exists a continuous transformation from a q satisfying (A23), when there will be no eigenvalues, to the given q, such that the intermediate q's are all non-negative, and, while q is changing, all the eigenvalues appear at $\lambda = 0$, and none disappear. It is thought that these conditions are met if q has a single maximum. (In that case suitable transformations are either increasing the height of q, or increasing the width of q, while keeping the shape of q constant.)

4. Special Initial Conditions

We end by giving the eigenvalues for our model initial conditions (22). Writing these in terms of q we have

$$q(\tau = 0, \xi) = B\,\mathrm{sech}(\xi)\exp(ik_0\xi)\,, \tag{A30}$$

where $B = A(\kappa/6)^{1/2}$. In this case the Zakharov-Shabat equations may be solved exactly in terms of hypergeometric functions.[17] The number of solitons is N, where $B = N + \varepsilon$, with $-\frac{1}{2} < \varepsilon \le \frac{1}{2}$. The eigenvalues are

$$\lambda_j = i\tfrac{1}{2}a_j - \tfrac{1}{2}k_j = i(\varepsilon - \tfrac{1}{2} + j) - \tfrac{1}{2}k_0\,, \quad \text{for } j = 1, 2, \ldots N\,. \tag{A31}$$

Because of the symmetry of $q(\tau = 0)$ in ξ we have

$$\beta(\lambda_j) = (-1)^{N-j+1}\,. \tag{A32}$$

The amount of radiation is then given by

$$\int_{-\infty}^{\infty} \tfrac{1}{2}|q_{\text{radiation}}|^2\, d\xi = \int_{-\infty}^{\infty} \tfrac{1}{2}|q(\tau = 0)|^2\, d\xi - \int_{-\infty}^{\infty} \tfrac{1}{2}|q_{\text{soliton}}(\tau \to \infty)|^2\, d\xi$$

$$= B^2 - 2\Sigma_j \operatorname{Im}(\lambda_j) = \varepsilon^2 \le \tfrac{1}{4}\,. \tag{A33}$$

Thus for B large the radiation is small compared with the soliton part of the solution. In particular, if B is an integer, N, then there is no radiation (since $\varepsilon = 0$). The sech pulse then represents an exact N-soliton collision. In this case the residues are found from (A8) and (A32) to be

$$\mu_j = -iN\,\Pi_{p<j}\,(N^2 - p^2)/p^2\,. \tag{A34}$$

From (A18) and (A19) the positions and phases of the solitons at $\tau \to \infty$ are

$$a_j\xi_j = -\log(N) + \Sigma_{p<j} \log[4(4p^2-1)/(N^2-p^2)]\,, \tag{A35}$$

$$\theta_j = 0\,. \tag{A36}$$

If we are not interested in the precise N-soliton solution for finite τ (A10) we may still identify the important time scales on which the solution evolves using the soliton velocities and frequencies (A16). We define two time scales: a filamentation time scale, τ_f, or the time it takes for two typical solitons to separate from one another; and a self-focussing time scale, τ_s, or the time for the relative phases of two typical solitons to change by π. For definiteness we take the two "typical" solitons to be the tallest one (index N) and the half tallest one (index $\frac{1}{2}N$; assume N is even). Assuming $B \gg 1$, we have

$$\tau_f = (a_N^{-1} + a_{N/2}^{-1})(c_N - c_{N/2})^{-1} \approx \tfrac{1}{2}B^{-3}\,, \tag{A37}$$

$$\tau_s = \pi(\omega_N - \omega_{N/2})^{-1} \approx \pi(9k_0B^2)^{-1}\,. \tag{A38}$$

Loosely speaking (A37) and (A38) give the times we have to wait to see the first effects of filamentation and self-focussing. We should not confuse τ_f with the time it takes for all the solitons to separate, which is a time of order unity for these initial conditions.

References

[1]G. J. Morales and Y. C. Lee, Phys. Rev. Lett. 35, 930 (1975).

[2]K. B. Dysthe, E. Mjølhus, H. Pécseli, and L. Stenflo, Report No. 50-78, University of Tromsø, Norway (1978).

[3]A. C. Scott, F. Y. F. Chu, and D. W. McLaughlin, Proc IEEE 61, 1443 (1973).

[4]M. J. Ablowitz, D. J. Kaup, A. C. Newell, and H. Segur, Stud. Appl. Math. 53, 249 (1974).

[5]G. L. Johnston, F. Y. F. Chu, C. F. F. Karney, and A. Bers, RLE-PRR 76/18-2, M.I.T. (1976).

[6]A. C. Newell and D. J. Kaup, Bull. Am. Phys. Soc. 21, 1095 (1976).

[7]R. Hirota, J. Math. Phys. 14, 805 (1973).

[8]H. H. Kuehl, Private Communication (1977).

[9]G. P. Leclert, C. F. F. Karney, A. Bers, and D. J. Kaup, RLE-PRR 77/25, M.I.T. (1977).

[10]H. Sanuki and T. Ogino, Phys. Fluids 20, 1510 (1977).

[11]A. Sen, C. F. F. Karney, G. L. Johnston, and A. Bers, Nucl. Fusion 18, 171 (1978).

[12]N. R. Pereira, A. Sen, and A. Bers, Phys Fluids 21, 117 (1978).

[13]G. J. Morales, Phys. Fluids 20, 1164 (1977).

[14]V. E. Zakharov and A. B. Shabat, Zh. Eksp. Teor. Fiz. 61, 118 (1971) [Sov. Phys. - JETP 34, 62 (1972)].

[15]M. Wadati, J. Phys. Soc. Japan 34, 1289 (1973).

[16]Y.-C. Ma, *Studies of the Cubic Schrödinger Equation*, Ph.D. Thesis, Department of Aerospace and Mechanical Sciences, Princeton University (1977).

[17]J. Satsuma and N. Yajima, Supp. Prog. Theor. Phys. 55, 284 (1974).

Figure Captions

Fig. 1. The results of numerically integrating the CMKDV equation. The initial condition is given by (22) with $A = 3$ and $k_0 = 1$. The figure shows v at (a) $\tau = 0$, (b) $\tau = 0.5$, (c) $\tau = 2$. The solid line gives $|v|$, the long dashes $\mathrm{Re}(v)$, and the short dashes $\mathrm{Im}(v)$. The numerical integration was performed with $L = 40$, $n = 2^8$, $\delta\tau = 5 \times 10^{-4}$. At $\tau = 2$ the errors are $\delta_2 = 3 \times 10^{-4}$, $\delta_3 = 4 \times 10^{-4}$.

Fig. 2. The same as Fig. 1, except $A = 5$, $k_0 = 3$, and $\delta\tau = 2 \times 10^{-4}$. (a) $\tau = 0$, (b) $\tau = 0.2$, (c) $\tau = 0.6$. ($\delta_2 = 2 \times 10^{-4}$, $\delta_3 = 10^{-4}$ at $\tau = 0.6$.)

Fig. 3. The collision of two constant phase pulses of the form (23). The taller one has $a = \sqrt{2}$, $\theta_0 = 0$, $\xi_0 = -7$. The shorter one has $a = 1/\sqrt{2}$, $\theta_0 = \frac{1}{2}\pi$, $\xi_0 = 7$. The integration is performed in a frame moving with velocity $1\frac{1}{4}$, the mean (initial) velocity of the pulses. Fig. 3(b) shows the result of the collision for the CMKDV equation, (c) the result for the MKDV equation. [$L = 30$, $n = 2^7$, $\delta\tau = 2 \times 10^{-3}$. In (b) $\delta_2 = 5 \times 10^{-5}$, $\delta_3 = 5 \times 10^{-5}$. In (c) $\delta_2 = 4 \times 10^{-5}$, $\delta_3 = 10^{-4}$.]

Fig. 4. Phases of two constant phase pulses before and after their collision as a function of the initial difference of phase between them, $\Delta\theta$. The ratio of heights was initially 2. Subscripts 1 and 2 refer to the taller and shorter pulses respectively. Subscripts i and f refer to the initial and final phases.

Fig. 5. Envelope pulses for $k_0/a = 0.5$ [(a) and (b)] and $k_0/a = 2$ [(c) and (d)]. The solid line shows the results of integrating (26) numerically. The dashed lines in (c) and (d) gives the asymptotic expressions (32) and (33). A constant has been added to the asymptotic result in (c), so that it can be distinguished from the numerical result. The jaggedness in the numerical results on the right in (d) arises because (26) was integrated numerically from left to right, and, due to numerical error, a growing solution is being picked up on the right.

Fig. 6. The area $\int_{-\infty}^{\infty} |V|\, d\zeta$ of envelope pulses as a function of k_0/a. The solid line gives the numerical result. The dashed line the asymptotic result from (34). The area of the constant phase pulses is shown by the arrow.

Fig. 7. The same as Fig. 2, except $A = 6$, $k_0 = 3$, and $\delta\tau = 2 \times 10^{-4}$. (a) $\tau = 0.2$, (b) $\tau = 0.6$, (c) $\tau = 0.8$. ($\delta_2 = 4 \times 10^{-3}$, $\delta_3 = 5 \times 10^{-3}$ at $\tau = 0.8$.)

Fig. 8. Schematic showing the numbers and types of solitary pulses produced when the initial conditions are given by (22). The cross-hatched region shows where a mixture of constant phase and envelope pulses are produced. The left boundary of this region is the dividing line between 1 and 0 envelope pulses and the right boundary is the dividing line between 1 and 0 constant phase pulses. This figure is only intended to give a rough idea of what pulses are produced. All dividing lines which have been drawn as straight should in fact be curved. In particular the horizontal lines should curve up towards the cross-hatched region.

Fig. 9. The reflectivity, R, as a function of τ_1 when the boundary condition is given by (41) with: (a) $A = 2$, $k_0 = 0$; (b) $A = 3$, $k_0 = 0$; (c) $A = 4$, $k_0 = 0$; (d) $A = 4$, $k_0 = 1$. The crosses show where the numerical scheme for solving the boundary value problem ceased to converge. ($L = 40$, $n = 2^8$, $\delta\tau = 10^{-3}$, $\varepsilon = 2\%$.)

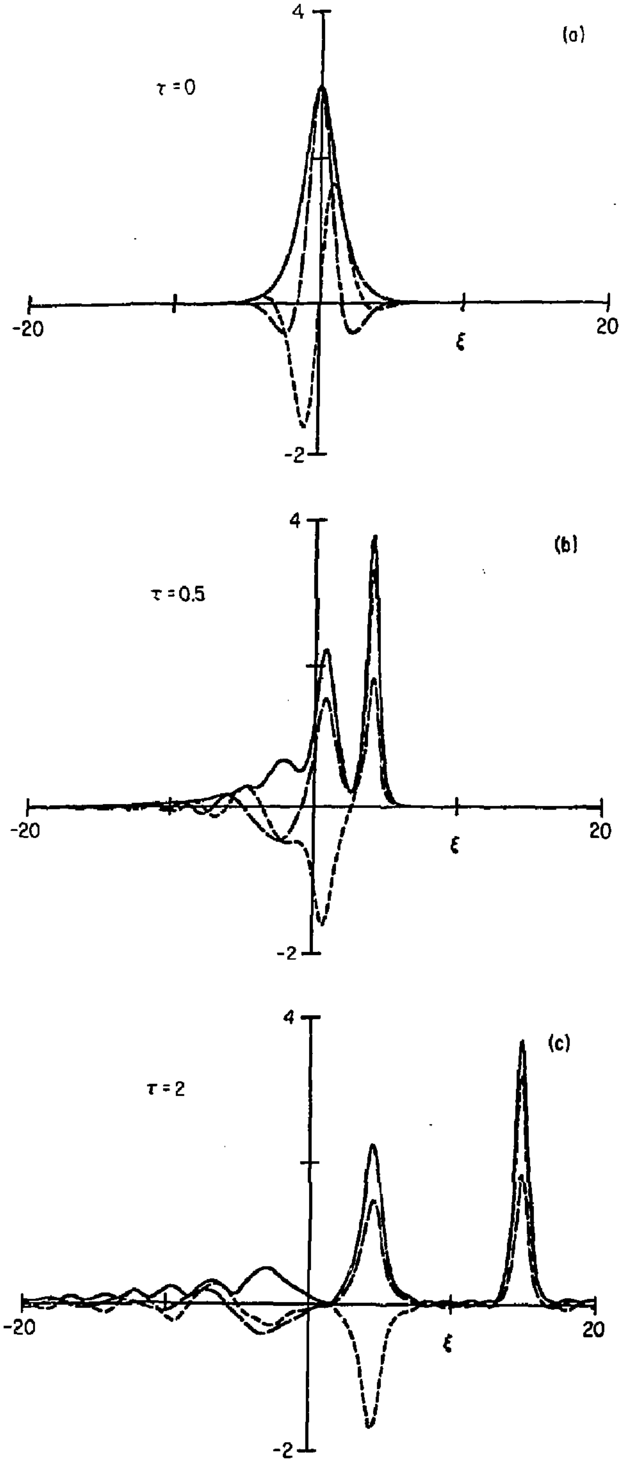

Fig. 1. 782165

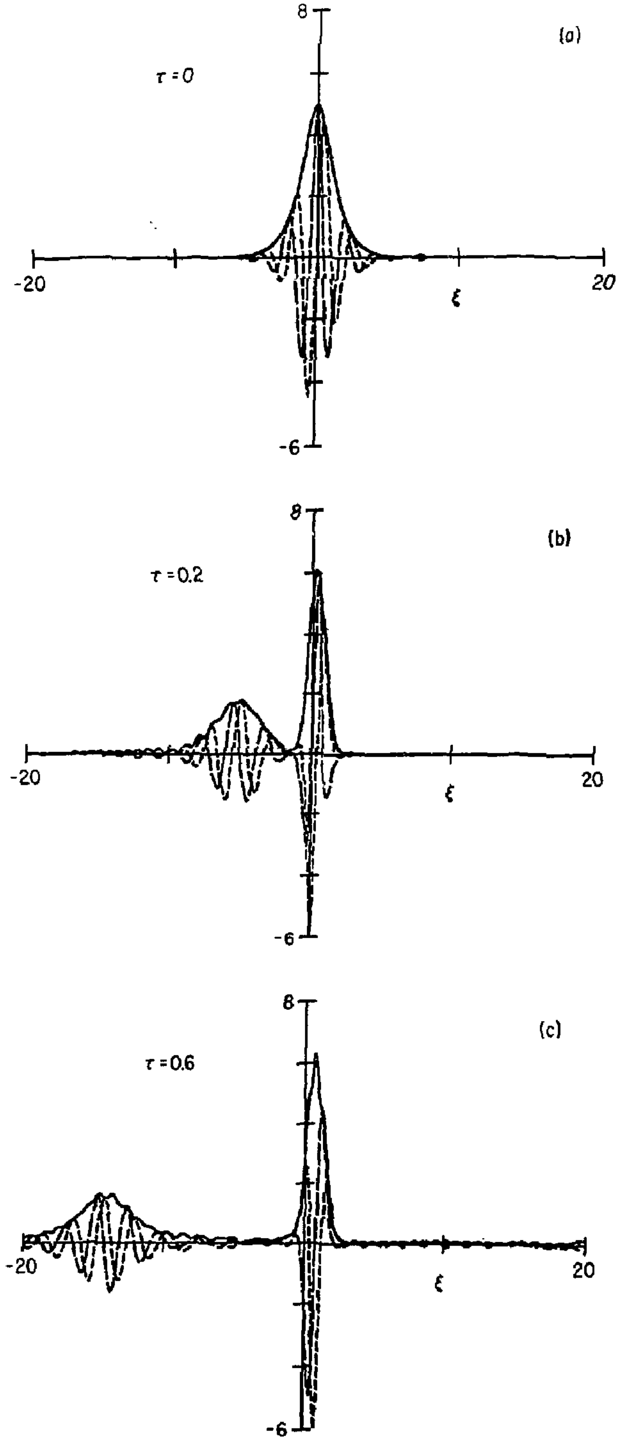

Fig. 2. 782166

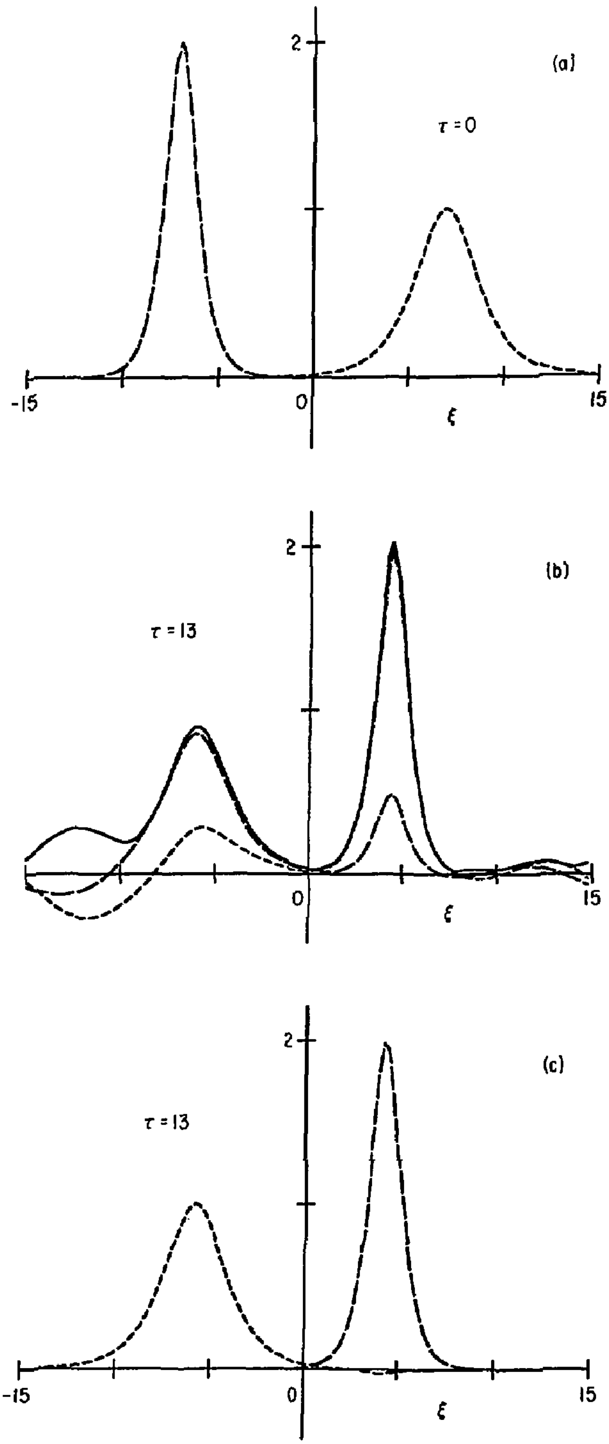

Fig. 3. 782164

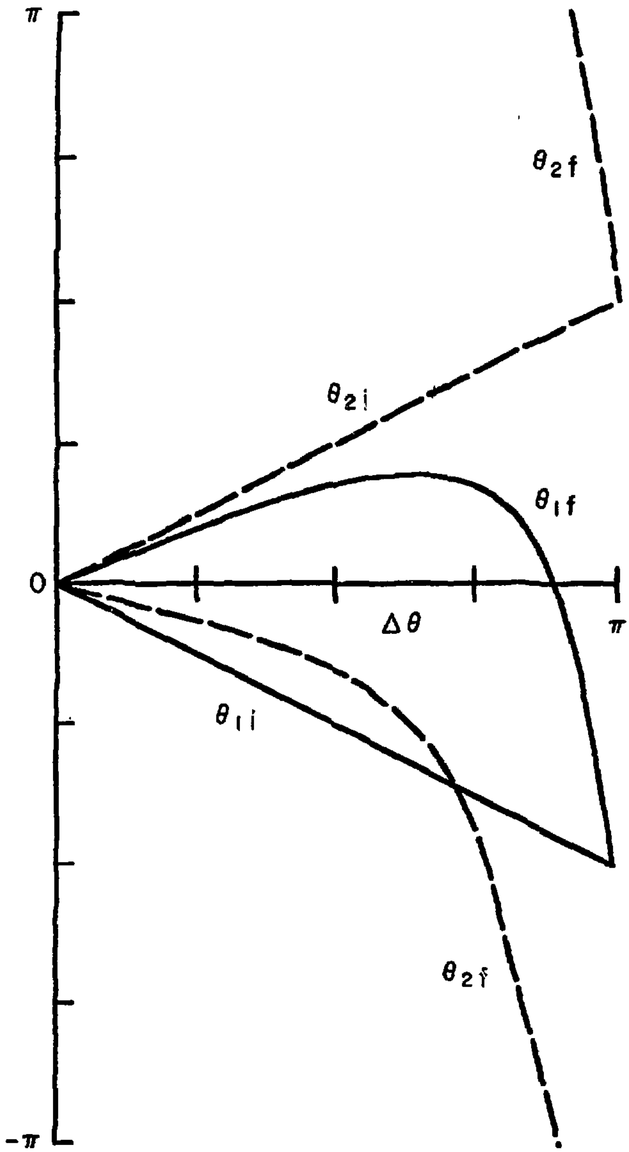

Fig. 4. 782161

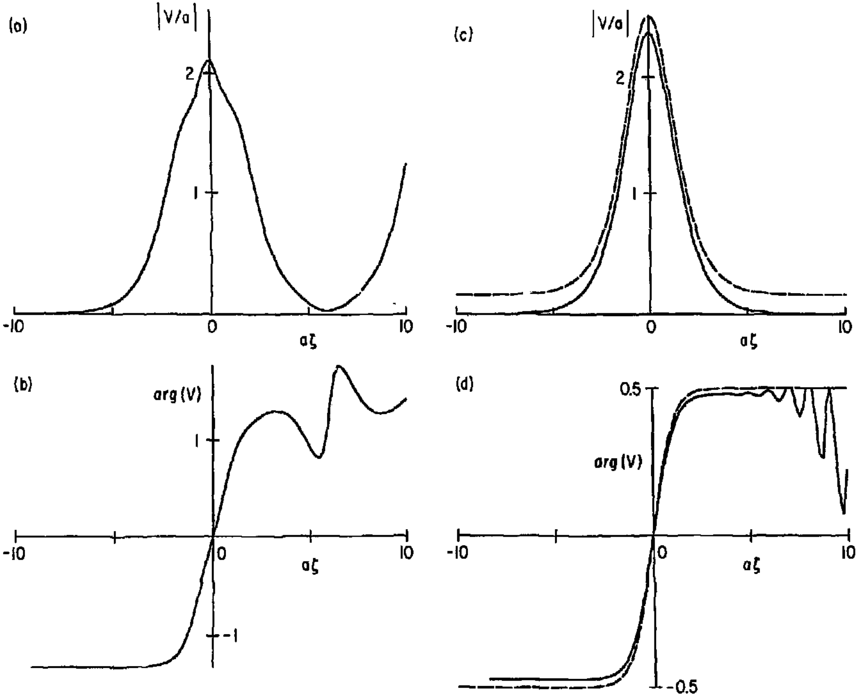
(a)
|V/a|
2
1
-10
0
10
aζ
(c)
|V/a|
2
1
-10
0
10
aζ
(b)
arg (V)
1
-1
-10
0
aζ
10
(d)
0.5
arg (V)
-10
0
aζ
10
-0.5

Fig. 5. 782167

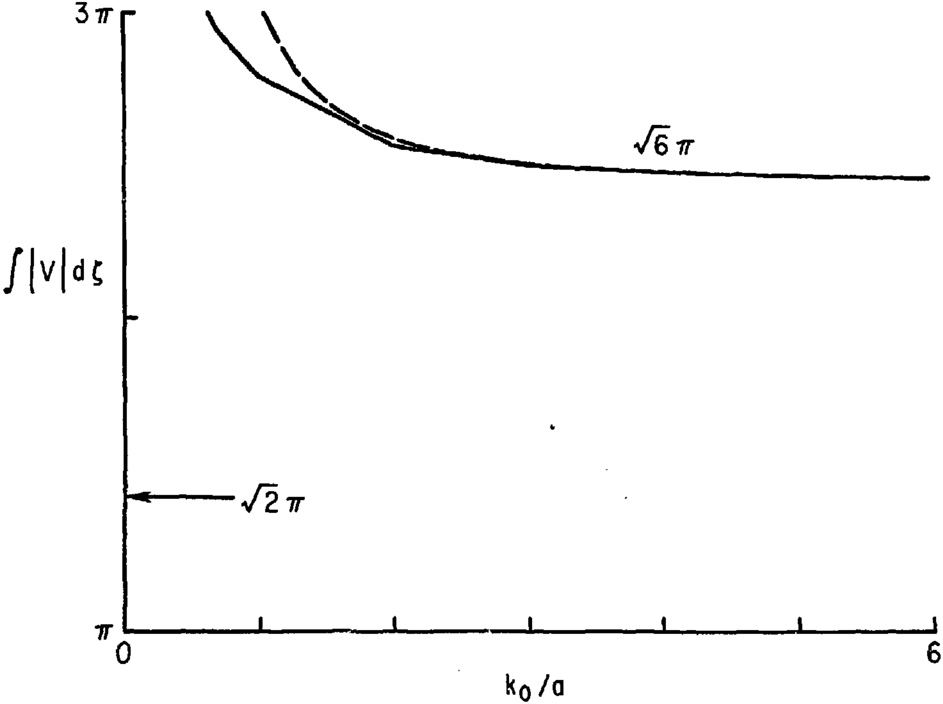

Fig. 6. 782162

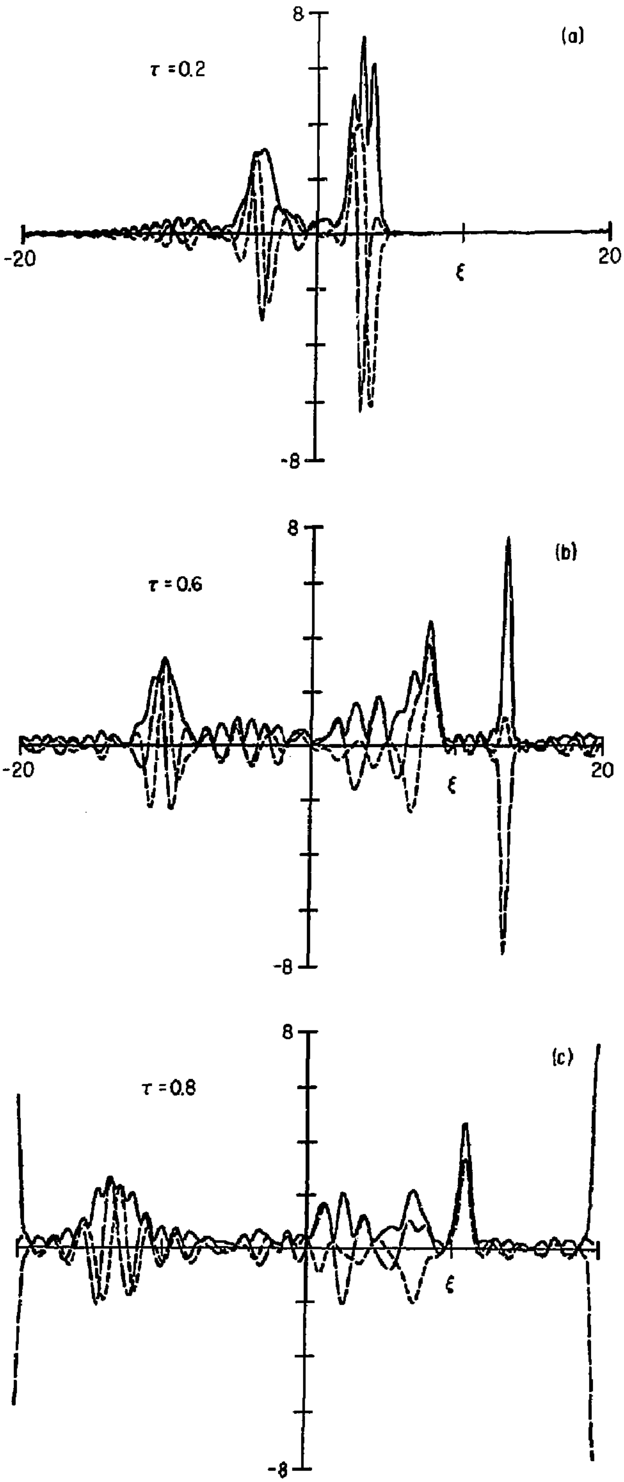

Fig. 7. 782163

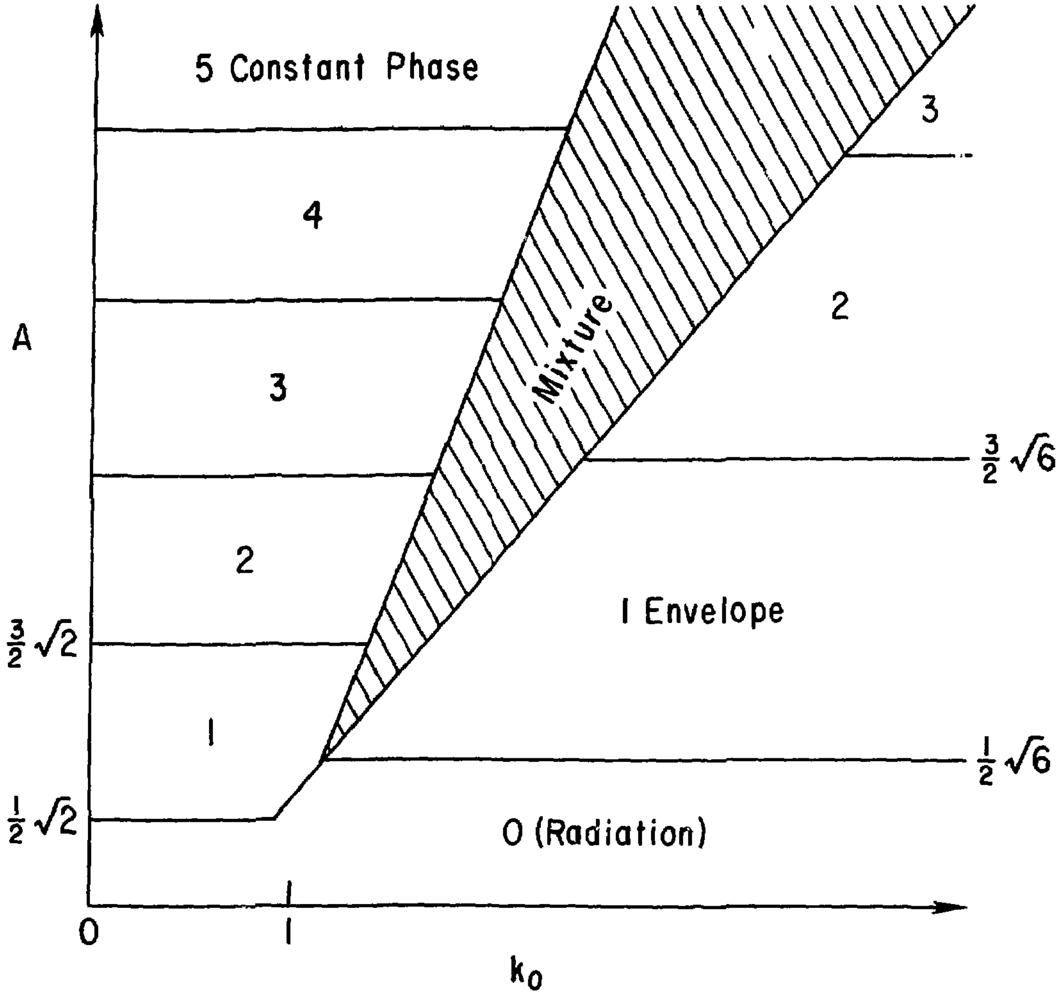
5 Constant Phase
4
3
2
1
A
$\frac{3}{2}\sqrt{2}$
$\frac{1}{2}\sqrt{2}$
Mixture
3
2
$\frac{3}{2}\sqrt{6}$
1 Envelope
$\frac{1}{2}\sqrt{6}$
0 (Radiation)
0
1
k_0

Fig. 8. 782159

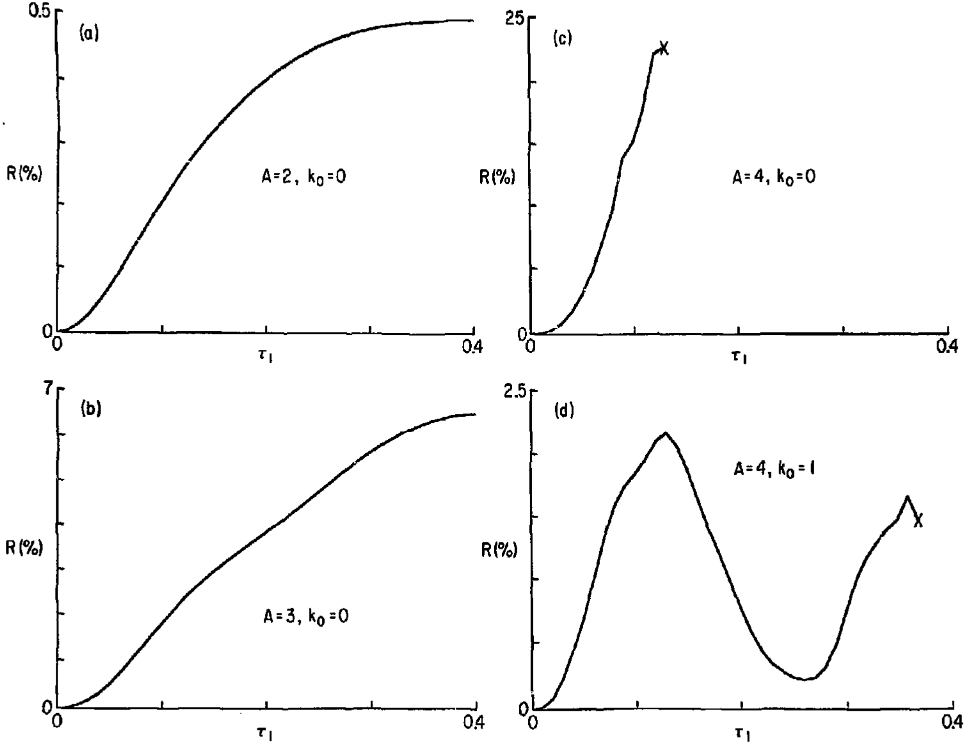

Fig. 9. 782160